

FTIR and XPS Study of Pt Nanoparticle Functionalization and Interaction with Alumina

Céline Dablemont,[†] Philippe Lang,[†] Claire Mangeney,[†] Jean-Yves Piquemal,[†]
Valeri Petkov,[‡] Frédéric Herbst,[†] and Guillaume Viau^{*,§}

Université Paris 7-Denis Diderot, ITODYS, UMR CNRS 7086, case 7090, 2 place Jussieu,
F-75251 Paris Cedex 05, France, Central Michigan University, Department of Physics, Mt. Pleasant,
Michigan 48859, and Université de Toulouse, INSA, LPCNO, UMR CNRS 5215, 135 av. de Rangueil,
31077 Toulouse Cedex 4, France

Received September 15, 2007. Revised Manuscript Received February 18, 2008

Platinum nanoparticles with a mean size of 1.7 nm were synthesized by reduction in sodium acetate solution in 1,2-ethanediol. The particles were then functionalized with dodecylamine, dodecanethiol, and ω -mercapto-undecanoic acid (MUDA). Fourier transform infrared (FTIR) spectroscopy and X-ray photoelectron spectroscopy (XPS) showed important variations of the particle surface state with functionalization whereas their structure differs only slightly. Platinum-to-sulfur charge transfer inferred from XPS of thiol-coated particles enabled the identification of the formation of Pt^{δ+}–S^{δ-} bonds. The native carbon monoxide (CO) at the surface of the particles was a very efficient probe for following the functionalization of the particles by FTIR. The red shift of $\nu(\text{CO})$ accounts for the nature of the ligands at the surface of the particles and also for their degree of functionalization. Immobilization on alumina substrates of particles functionalized with MUDA was realized by immersion in colloidal solutions. Free molecules, isolated particles, and aggregates of particles interconnected by hydrogen bonds at the surface of alumina were evidenced by FTIR. With successive washings, the energy variation of the CO stretch of carbon monoxide and of carboxylic acid groups and the relative intensity $\nu(\text{CH}_2)/\nu(\text{CO})$ showed that the free molecules are eliminated first, followed by aggregates and less-functionalized particles. Particles presenting a high degree of functionalization by MUDA remain and interact strongly with alumina.

Introduction

Metal nanoparticles present several applications in heterogeneous catalysis¹ or chemical sensors.² Platinum particles in particular are developed for their electrocatalytic activity in fuel cells.³ Size effects are very important both for catalytic activity and for electronic properties.⁴ Particle shape may also have a strong influence; for example, the catalytic activity of multifaceted tetrahedral platinum nanocrystals prepared by electrochemical techniques was found to be enhanced by up to 400% compared to that of spheres in the catalytic electro-oxidation of formic acid.^{3a} Liquid-phase processes are generally more interesting than other methods for very good control of size and shape.⁵ Several methods have been studied with respect to the synthesis of ultrafine Pt nanoparticles by reduction with hydrides in polar and nonpolar solvents,^{6,7} in microemulsions,⁸ by reduction in

ethylene glycol,^{9,10} or by the decomposition of organometallic precursors in the presence of a stabilizing agent¹¹ or in ionic liquids.¹² The reduction of platinum salts in polyvinyl pyrrolidone solution in ethylene glycol lead to various shapes such as spheres,¹³ cubes,¹⁴ and tetrapods.¹⁵ Generally, the use of polymers or capping agents such as thiols⁶ and amines¹⁶ is required to prevent the nanoparticles from coalescing. Furthermore, the functionalization of metal particles with ligands allowed their immobilization on oxides and could be promising for the use of metal colloids in heterogeneous catalysis.¹⁷

Besides catalytic applications, metal nanoparticles are also investigated for potential uses in solid state electronic devices. Two-dimensional assemblies of monodisperse metal particles with controlled size in the nanometer range present considerable interest in various applications of nanophysics: surface plasmon resonance,¹⁸ magnetic properties for ultrahigh density media

* guillaume.viau@insa-toulouse.fr.

[†] Université Paris 7.

[‡] Central Michigan University.

[§] Université de Toulouse.

(1) (a) Somorjai, G. A. *Introduction to Surface Chemistry and Catalysis*, Wiley, NY, 1994. (b) Ikeda, S.; Ishino, S.; Harada, T.; Okamoto, N.; Sakata, T.; Mori, H.; Kuwabata, S.; Torimoto, T.; Matsumura, M. *Angew. Chem., Int. Ed.* **2006**, *45*, 7063. (c) Sharma, G.; Mei, Y.; Lu, Y.; Ballauff, M.; Irrgang, T.; Proch, S.; Kempe, R. *J. Catal.* **2007**, *246*, 10. (d) Mandal, S.; Roy, D.; Chaudhari, R. V.; Sastry, M. *Chem. Mater.* **2004**, *16*, 3714.

(2) (a) Krasteva, N.; Besnard, I.; Guse, B.; Bauer, R. E.; Mullen, K.; Yasuda, A.; Vossmeier, T. *Nano Lett.* **2002**, *2*, 551. (b) Leopold, M. C.; Donkers, R. L.; Georganopolou, D.; Fisher, M.; Zamborini, F. P.; Murray, R. W. *Faraday Discuss.* **2004**, *125*, 63.

(3) (a) Tian, N.; Zhou, Z.-Y.; Sun, S.-G.; Ding, Y.; Wang, Z. L. *Science* **2007**, *316*, 732. (b) Kongkanand, A.; Kuwabata, S.; Girishkumar, G.; Kamat, P. *Langmuir* **2006**, *22*, 2392. (c) Jiang, S. P.; Liu, Z.; Tang, H. L.; Pan, M. *Electrochim. Acta* **2006**, *51*, 5721. (d) Che, G.; Lakshmi, B. B.; Fisher, E. R.; Charles, R. *Nature* **1998**, *393*, 346.

(4) Arenz, M.; Mayrhofer, K. J. J.; Stamenkovic, V.; Blizanac, B. B.; Tomoyuki, T.; Ross, P. N.; Markovic, N. M. *J. Am. Chem. Soc.* **2005**, *127*, 6819.

(5) Park, J.; Joo, J.; Kwon, S. G.; Jang, Y.; Hyeon, T. *Angew. Chem., Int. Ed.* **2007**, *46*, 4630.

(6) Yang, J.; Lee, J. Y.; Deivaraj, T. C.; Too, H. P. *Langmuir* **2003**, *19*, 10361.

(7) Eklund, S. E.; Cliffl, D. E. *Langmuir* **2004**, *20*, 6012.

(8) Ingelsten, H. H.; Bagwe, R.; Palmqvist, A.; Skoglundh, M.; Svanberg, C.; Holmberg, K.; Shah, D. O. *J. Colloid Interface Sci.* **2001**, *241*, 104.

(9) (a) Viau, G.; Toneguzzo, P.; Pierrard, A.; Acher, O.; Fiévet-Vincent, F.; Fiévet, F. *Scr. Mater.* **2001**, *44*, 2263. (b) Yang, J.; Deivaraj, T. C.; Too, H. P.; Lee, J. Y. *Langmuir* **2004**, *20*, 4241.

(10) Wang, Y.; Ren, J.; Deng, K.; Gui, L.; Tang, Y. *Chem. Mater.* **2000**, *12*, 1622.

(11) Dassenoy, F.; Philippot, K.; Ould-Ely, T.; Amiens, C.; Lecante, P.; Snoeck, E.; Mosset, A.; Casenove, M.-J.; Chaudret, B. *New J. Chem.* **1998**, *22*, 703.

(12) Scheeren, C. W.; Machado, G.; Teixeira, S. R.; Morais, J.; Domingos, J. B.; Dupont, J. *J. Phys. Chem. B* **2006**, *110*, 13011.

(13) Bonet, F.; Tekaiia-Elhissen, K.; Sarathy, K. V. *Bull. Mater. Sci.* **2000**, *23*, 165.

(14) Song, H.; Kim, F.; Connor, S.; Somorjai, G. A.; Yang, P. *J. Phys. Chem. B* **2005**, *109*, 188.

(15) Chen, J.; Herricks, T.; Xia, Y. *Angew. Chem., Int. Ed.* **2005**, *44*, 2589.

(16) Yang, J.; Deivaraj, T. C.; Too, H. P.; Lee, J. Y. *J. Phys. Chem. B* **2004**, *108*, 2181.

(17) (a) Yu, W.; Liu, M.; Liu, H.; An, X.; Liu, Z.; Ma, X. *J. Mol. Catal. A* **1999**, *142*, 201. (b) Brayner, R.; Viau, G.; Bozon-Verduraz, F. *J. Mol. Catal. A* **2002**, *182–183*, 227.

storage,¹⁹ and transport properties²⁰ and in electronic devices such as new flash memories.²¹ A new concept of a voltage-controlled variable capacitor has been proposed recently.²² These devices consist of a 2D assembly of conducting nanoparticles embedded in a thin insulating layer of a plane capacitor. The transport properties of such capacitors rely on Coulomb blockade in the 2D nanoparticle assembly.²² The successful combination of physical and chemical means for the realization of variable capacitors has been shown recently.²³ The first results were obtained with 3 nm ruthenium particles,²³ but the next challenge is to lower the particle size to below 1.5 nm in order to increase the working temperature up to room temperature.²²

The integration of "chemical particles" in solid state devices for electronic applications requires not only control over their mean size and the precise study of their chemical environment as for heterogeneous catalysis but also control over their organization in 1D, 2D, or 3D arrays onto substrates. Several methods have been studied to produce 2D superlattices on oxide surfaces either by self-organization processes obtained after evaporation²⁴ or by grafting the particles onto chemically modified surfaces. The silanization of oxide surfaces with amino- or mercaptosilane is one of the most well studied methods for this purpose.²⁵ The Langmuir-Blodgett technique is very interesting for a strictly 2D assembly.²⁶ The covalent immobilization of gold colloids onto self-assembled monolayers (SAMs) has also been proposed.²⁷ Metal nanoparticles/polyelectrolyte ultrathin films can be grown as well by layer-by-layer self-assembly methods through electrostatic interactions.²⁸

In this article, we describe the synthesis of platinum nanoparticles with a mean size of less than 2 nm. We report on their functionalization by dodecylamine, dodecanethiol, and ω -mercaptoundecanoic acid (MUDA). We also report on the immobilization of these particles onto alumina surfaces. We show that X-ray photoelectron spectroscopy (XPS) and Fourier transform infrared (FTIR) spectroscopy are very useful in describing the particle surface modification with functionalization and in following their interaction with alumina.

Experimental Section

Synthesis. Platinum nanoparticles were prepared by the reduction of potassium tetrachloroplatinate (K_2PtCl_4) or by the reduction of dihydrogen hexachloroplatinate hydrate (H_2PtCl_6) in a hot sodium acetate solution in 1,2-ethanediol. The platinum salt concentration was 3 mM, and the temperature fixed at 80 °C. The platinum particles

were functionalized either with dodecylamine, dodecanethiol, or ω -mercaptoundecanoic acid (MUDA). In the two first cases, the nanoparticles were extracted from polyol into a 3 mM solution of dodecylamine or dodecanethiol in toluene. After 1 night, the extraction was complete, and brown colloidal solutions were obtained.

Particles were coated with MUDA by adding 0.5 equiv of the mercapto acid, with respect to atomic platinum, to the cold polyol solution containing the platinum particles and stirring this solution for 1 night. The particles were flocculated by adding two volumes of water, and the precipitate was washed with water. Platinum particles coated with MUDA were then redispersed under sonication in absolute ethanol or in 3 mM chlorhydric acid solution in ethanol to increase the colloidal solution stability.

Immobilization on an Alumina Surface. Alumina thin layers (thicknesses of 3 and 6 nm) were deposited by sputtering a stoichiometric alumina crucible with a Plassys apparatus, either on copper grids for transmission electron microscope studies (3 nm) or on silicon wafers for XPS and infrared absorption spectroscopy (6 nm). Unless specified, both alumina-covered copper grids and silicon wafers have been treated with 98% sulfuric acid to remove any organic contaminant and washed abundantly with ultrapure water and ethanol. The alumina surfaces were immersed in a solution containing platinum nanoparticles coated with MUDA for 1 night and then washed abundantly with ethanol. To improve the washings, alumina-covered silicon wafers have been sonicated in ethanol. Membranes (3 nm thick) on copper grids were useful for electron microscope observations. Unfortunately, these membranes are very fragile and are not resistant to sonication. Thus, the influence of washing has been studied only on alumina-covered silicon wafers.

Characterization. Transmission electron microscope (TEM) observations were carried out with a Jeol 100 kV JEM-100CX II microscope. High-resolution transmission electron microscopy was performed with a Jeol JEM 2010F UHR operating at 200 kV. One drop of a dilute colloidal solution of thiol-capped particles in toluene was deposited onto the amorphous carbon membrane of the transmission electron microscope grid, and the solvent was then evaporated at room temperature. In the case of particles coated with MUDA, 3-nm-thick alumina membranes deposited by sputtering on copper grids for transmission electron microscopy were used. The grids were immersed in the solutions as described in the previous section.

High-energy XRD experiments were carried out at the 11-ID-C beamline (Advanced Photon Source, Argonne National Laboratory) using synchrotron radiation of energy 115.243 keV ($\lambda = 0.10759$ Å) at room temperature. Synchrotron radiation X-rays were employed for two reasons. First, the high flux of synchrotron radiation X-rays allowed the measurement of the quite diffuse XRD pattern of Pt nanoparticles with very good statistical accuracy. Second, the high energy of synchrotron radiation X-rays permitted the collection of data over a wide range ($1-30$ Å⁻¹) of scattering vectors. Both are important for the success of the atomic PDF data analysis employed here. Pt nanoparticles were extracted from polyol to a toluene solution containing dodecylamine or dodecanethiol. Toluene was then evaporated, and the coated particles were washed several times with ethanol to remove excess surfactant. Dry nanoparticles were sandwiched between Kapton foils and measured in transmission geometry. Scattered radiation was collected with a large-area image plate detector (mar345). Five images were taken for each of the samples. The corresponding images were combined, subjected to geometrical corrections, reduced to structure factors, and Fourier transformed to atomic PDFs, $G(r) = 4\pi r[\rho(r) - \rho_0]$. Herein, $\rho(r)$ and ρ_0 represent the local and average atomic number densities, respectively, and r is the radial distance.

X-ray photoelectron spectra were recorded using a Thermo VG Scientific ESCALAB 250 system fitted with a microfocussed, monochromatic Al K α X-ray source (1486.6 eV) and a magnetic lens that increases the electron acceptance angle and hence the sensitivity. An X-ray beam of 650 μ m size was used (15 kV \times 200 W). The pass energy was set at 150 and 40 eV for the survey and the narrow regions, respectively. An electron flood gun was used, under a 2×10^{-8} mbar partial pressure of argon, for static charge

(18) (a) Hutter, E.; Fendler, J. H.; Roy, D. *J. Phys. Chem. B* **2001**, *105*, 11159.

(b) Laurent, G.; Felidj, N.; Aubard, J.; Levi, G.; Krenn, J. R.; Hohenau, A.; Schider, G.; Leitner, A.; Aussenegg, F. R. *J. Chem. Phys.* **2005**, *122*, 11102.

(19) Sun, S.; Murray, C. B.; Weller, D.; Folks, L.; Moser, A. *Science* **2000**, *287*, 1989.

(20) (a) Fendler, J. H. *Chem. Mater.* **2001**, *13*, 3196. (b) Ohgi, T.; Fujita, D. *Surf. Sci.* **2003**, *532-535*, 294.

(21) Paul, S.; Pearson, C.; Molloy, A.; Cousins, M. A.; Green, M.; Koliopoulou, S.; Dimitrakis, P.; Normand, P.; Tsoukalas, D.; Petty, M. C. *Nano Lett.* **2003**, *3*, 533.

(22) Seneor, P.; Lidgi, N.; Carrey, J.; Jaffrès, H.; Nguyen Van Dau, F.; Friederich, A.; Fert, A. *Europhys. Lett.* **2004**, *65*, 699.

(23) Lidgi-Guigui, N.; Dablemont, C.; Veautier, D.; Viau, G.; Seneor, P.; Nguyen Van Dau, F.; Mangeney, C.; Vaurès, A.; Deranlot, C.; Friederich, A. *Adv. Mater.* **2007**, *19*, 1729.

(24) Lin, X. M.; Jaeger, H. M.; Sorensen, C. M.; Klabunde, K. J. *J. Phys. Chem. B* **2001**, *105*, 3353.

(25) (a) Freeman, R. G.; Grabar, K. C.; Allison, K. J.; Bright, R. M.; Davis, J. A.; Guthrie, A. P.; Hommer, M. B.; Jackson, M. A.; Smith, P. C.; Walter, D. G.; Natan, M. J. *Science* **1995**, *267*, 1629. (b) Liu, Z.; Zhu, T.; Hu, R.; Liu, Z. *Phys. Chem. Chem. Phys.* **2002**, *4*, 6059. (c) Pavlovic, E.; Quist, A. P.; Gelius, U.; Oscarsson, S. *J. Colloid Interface Sci.* **2002**, *254*, 200.

(26) (a) Perez, H.; Lisboa de Sousa, R. M.; Pradeau, J.-P.; Albouy, P.-A. *Chem. Mater.* **2001**, *13*, 1512. (b) Raynal, F.; Etcheberry, A.; Cavaliere, S.; Noël, V.; Perez, H. *Appl. Surf. Sci.* **2006**, *252*, 2422.

(27) Chan, E. W. L.; Yu, L. *Langmuir* **2002**, *18*, 311.

(28) Cassagneau, T.; Fendler, J. H. *J. Phys. Chem. B* **1999**, *103*, 1789.

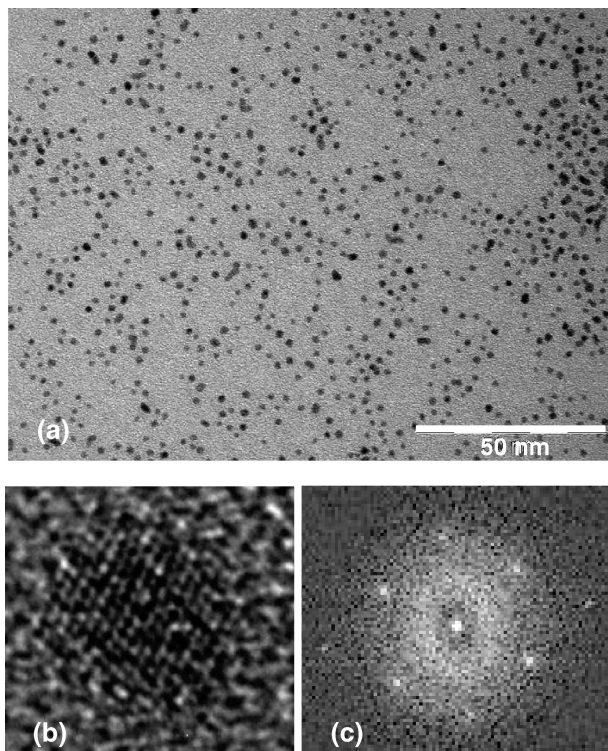


Figure 1. (a) Transmission electron microscopy of platinum nanoparticles prepared by the reduction of K_2PtCl_4 in 1,2-ethanediol and then by coating with dodecanethiol ($d_m = 1.7$ nm; $\sigma = 0.4$ nm). (b) High-resolution image of a single particle and (c) numerical electron diffraction pattern indexed as the [011] zone axis.

compensation. These conditions resulted in negative but uniform static charge. Spectral calibration was determined by setting the main C 1s component at 285 eV. Avantage software, version 2.2, was used for digital acquisition and data processing. The surface composition was determined using the integrated peak areas, and the corresponding Scofield sensitivity factors were corrected for the analyzer transmission function. The Pt 4f signal was fitted using asymmetric peaks to account for multiplet splitting. For XPS analysis, the coated particles were recovered (i) either by evaporating the solvent of the colloidal solutions and further washing with ethanol in the case of dodecylamine and dodecanethiol coated particles or (ii) by flocculating with water in the case of MUDA-coated particles. All particles were then dried in air at 50 °C.

Infrared ATR spectra were recorded on a Nicolet 860 Fourier transform infrared (FTIR) (Thermo Electron) spectrometer with a resolution of 4 cm^{-1} by adding 500 scans. The ATR configuration was used with a 45° angle of incidence $39 \times 15 \times 0.4\text{ mm}^3$ silicon crystal (48 internal reflections on each face.) The crystals were cut from n-doped silicon wafers (Siltronix; resistivity $\approx 150\ \Omega\cdot\text{cm}$). Spectra were run in a sample compartment flushed for 20 min with dry air. They were referenced to a background spectrum previously recorded on the crystal without the nanoparticles and cleaned under the same conditions as for the covered crystal. Two kinds of analysis were realized. One drop of the solution of particles in polyol or coated with organic ligands was deposited on a silicon substrate, and the solvent was evaporated at room temperature. Particles immobilized by immersion on the alumina layer deposited on a silicon wafer as described above were also analyzed, and in that case, the influence of washing was studied.

Results and Discussion

Morphology and Structure of Pt Nanoparticles. The best conditions for getting nonagglomerated platinum particles with a mean size below 2 nm were obtained with K_2PtCl_4 as the precursor and with a sodium acetate concentration of 10 mM.

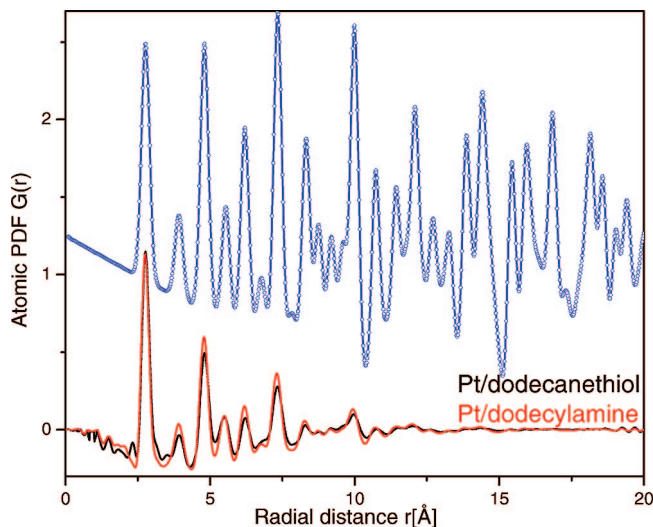


Figure 2. Experimental atomic PDFs for Pt nanoparticles prepared by the reduction of K_2PtCl_4 and coated with dodecylamine (red line) and with dodecanethiol (black line). A theoretical PDF for bulk Pt is shown (blue symbols) shifted up for clarity.

Such particles coated with dodecanethiol are well dispersed on the microscope carbon grid (Figure 1a). The mean diameter (d_m) and standard deviation (σ) of the size distribution estimated from the image analysis of ca. 250 particles were found to be $d_m = 1.7$ nm and $\sigma = 0.4$ nm. When H_2PtCl_6 was used as the precursor, the standard deviation was always found to be slightly higher with a higher population of elongated particles.

Experimental atomic PDFs for dry Pt particles are shown in Figure 2. The PDFs exhibit a series of well-defined peaks, with each corresponding to a frequently occurring interatomic distance. The first peak in the experimental PDFs is positioned at $2.77\ \text{Å}$, which is the first atomic neighbor distance in bulk (zero valent) Pt. All peaks in the experimental PDFs follow a sequence observed in the fcc-type structure.²⁹ The experimental PDFs for both amine- and thiol-covered Pt particles, however, decay to zero much faster than a PDF for a 2 nm piece of bulk Pt would (Figure 2). This rapid decay indicates that the fcc-type atomic ordering in the nanoparticles is not as perfect as in the corresponding bulk material. From the two types of nanoparticles studied, those covered with thiol show a length of structural coherence that is slightly shorter than that in the amine-covered particles. The presence of strain and local structural disorder, which is often due to surface relaxation, is a common phenomenon in particles of only a few nanometers in size. High-resolution electron microscopy on isolated monocrystalline particles confirmed the fcc structure with a diffraction pattern indexed as the [011] zone axis of the fcc structure (Figure 1b,c).

Colloidal solutions of MUDA-functionalized platinum particles in neutral ethanol tend to flocculate with time, and particles could be recovered from these solutions by 15 000 rpm centrifugation for 5 min. After the addition of 1 or 2 equiv (with respect to MUDA) of chlorhydric acid to the colloidal suspensions in ethanol, centrifugation is no more efficient in recovering platinum particles, showing a stabilizing effect. This difference was confirmed by transmission electron microscopy. TEM images recorded after one drop of neutral colloidal solution being deposited on the carbon grid show that particles tend to form aggregates of several tens of particles (Figure 3a). After acidification of the solution, the TEM images show much more isolated particles on the carbon grid (Figure 3b).

(29) X-ray powder data file J.C.PDS No. 00-004-0802.

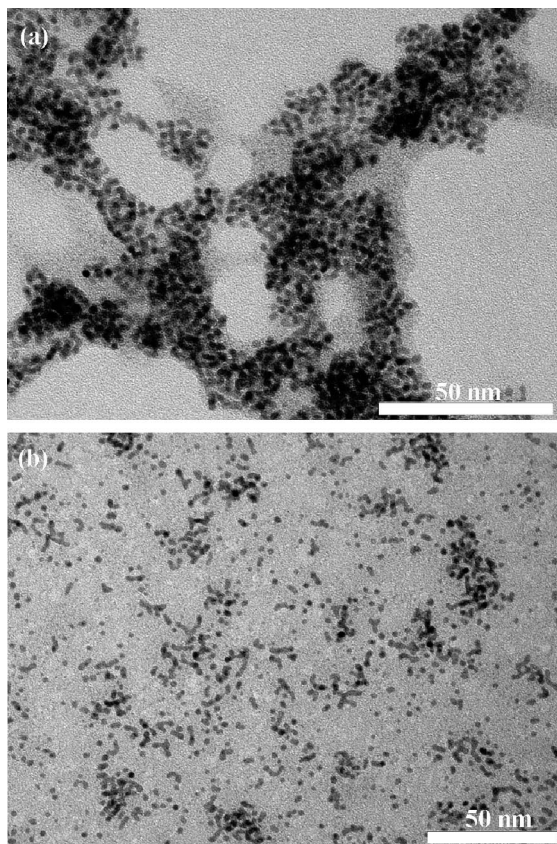


Figure 3. TEM image of Pt particles prepared by the reduction of H_2PtCl_6 and coated with MUDA: deposited on a carbon membrane from a neutral ethanol suspension (a) and after the addition of 1 equiv of chlorhydric acid in the suspension (b).

XPS and FTIR Study of Pt Nanoparticle Functionalization

XPS. X-ray photoelectron spectroscopy was performed on particles recovered after the evaporation of toluene in the case of dodecylamine- and dodecanethiol-coated particles or after flocculation in water and washing with ethanol, followed by centrifugation in the case of MUDA-coated particles.

The main peaks observed in the survey scans of the different samples are C 1s, Pt 4f, and O 1s peaks centered at ca. 285, 72, and 530 eV, respectively. For the thiol-capped particles and for the amine-capped particles, the S 2p peak at ca. 163 eV and the N 1s peak at ca. 400 eV, respectively, were also observed.

The binding energy of Pt 4f_{7/2} in the XPS spectra of the amine-coated particles was 71.2 eV (fwhm = 1.2 eV), corresponding to platinum in the zero-valent state.³⁰ The same peak broadens significantly in the spectra of dodecanethiol-coated particles. The main contribution is also located at 71.0 eV (fwhm = 1.3 eV), but an additional contribution at 72.1 eV (fwhm = 1.3 eV) was necessary to fit the experimental Pt 4f_{7/2} peak correctly (Figure 4). The energy shift is much lower than that recorded for the potassium tetrachloroplatinate in which platinum is in the 2+ valence state, $\Delta E = 2.4$ eV with respect to Pt(0).³¹ It is also lower than the binding energy of the platinum oxides PtO and PtO₂, observed on partially oxidized nanoparticles.^{30,32} The contribution at higher energy is attributed to the surface platinum atoms linked to the sulfur atom of dodecanethiol. XPS provides valuable information on the charge transfer between metals and

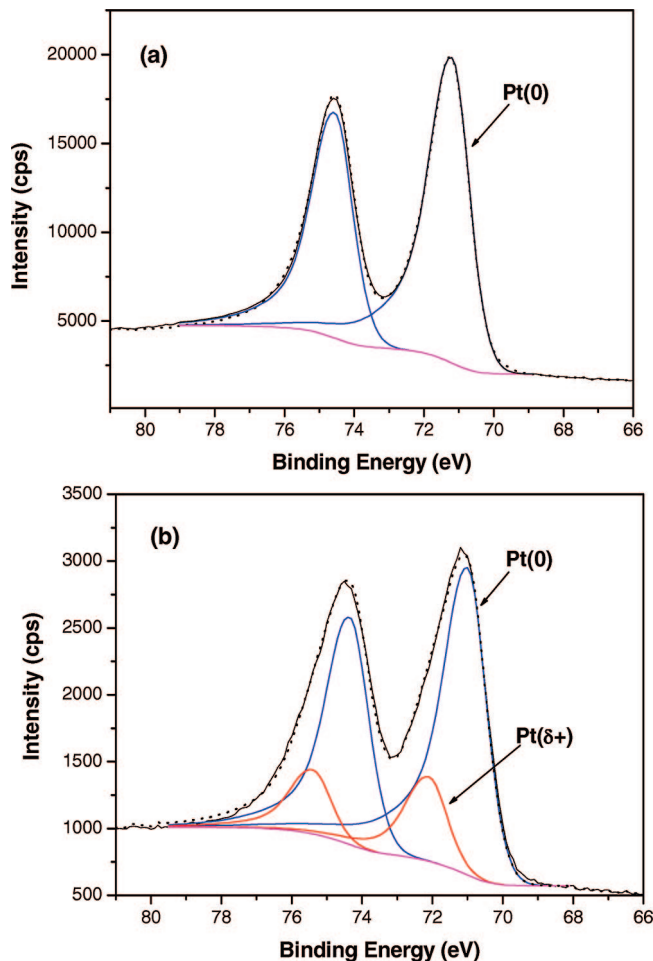


Figure 4. Pt 4f_{7/2} and 4f_{5/2} XPS spectra of platinum nanoparticles prepared by the reduction of K_2PtCl_4 in 1,2-ethanediol and coated with (a) dodecylamine and (b) dodecanethiol. The fwhm values of the peaks given by the fit are (a) 1.2 and (b) 1.3 eV.

adsorbed ligands at their surface.³³ Previous studies showed an influence of the organic ligand on the Pt 4f binding energy of platinum nanoparticles.^{34,35} The Pt–S charge transfer in the thiol-coated particles is more important than the Pt–N one in the amine-coated particles and is responsible for the energy shift. It must be stressed that this effect is observable in very fine particles with a mean diameter below 2 nm but is more difficult to detect on films. The area corresponding to the peak of platinum in the high valence state reaches 20% of the total area. For such Ultrafine particles coated with a 1.5-nm-thick layer of organic molecules, one can consider that the depth probed by XPS involves the whole platinum particle from the core to the surface. For a diameter of 2 nm, one can estimate that a particle contains 300 atoms, with a proportion of surface atoms of about 50%.³⁶ These values show that less than one-half of the platinum surface atoms are bound to dodecanethiol.

Two powders of MUDA-coated particles have been analyzed by XPS. For the first one (noted Pt-MUDA 1), both the contact time in polyol between MUDA and platinum particles and the delay between functionalization and XPS analysis have been short (respectively 1 night and several hours). For the second

(30) NIST X-ray Photoelectron Spectroscopy Database; data compiled and evaluated by Wagner, C. D.; Naumkin, A. V.; Kraut-Vass, A.; Allison, J. W.; Powell, C. J.; Rumble, J. R. <http://srdata.nist.gov/xps/>.

(31) Karpov, A.; Konuma, M.; Jansen, M. *Chem. Commun.* **2006**, 838.

(32) Sen, F.; Gökağç, G. *J. Phys. Chem. C* **2007**, *111*, 5715.

(33) Qiu, L.; Liu, F.; Zhao, L.; Yang, W.; Yao, J. *Langmuir* **2006**, *22*, 4480.
(34) Fu, X.; Wang, Y.; Wu, N.; Gui, L.; Tang, Y. *J. Colloid Interface Sci.* **2001**, *243*, 326.

(35) Tu, W.; Takai, K.; Fukui, K.; Miyazaki, A.; Enoki, T. *J. Phys. Chem. B* **2003**, *107*, 10134.

(36) Van Hardeveld, R.; Hartog, F. *Surf. Sci.* **1969**, *15*, 189.

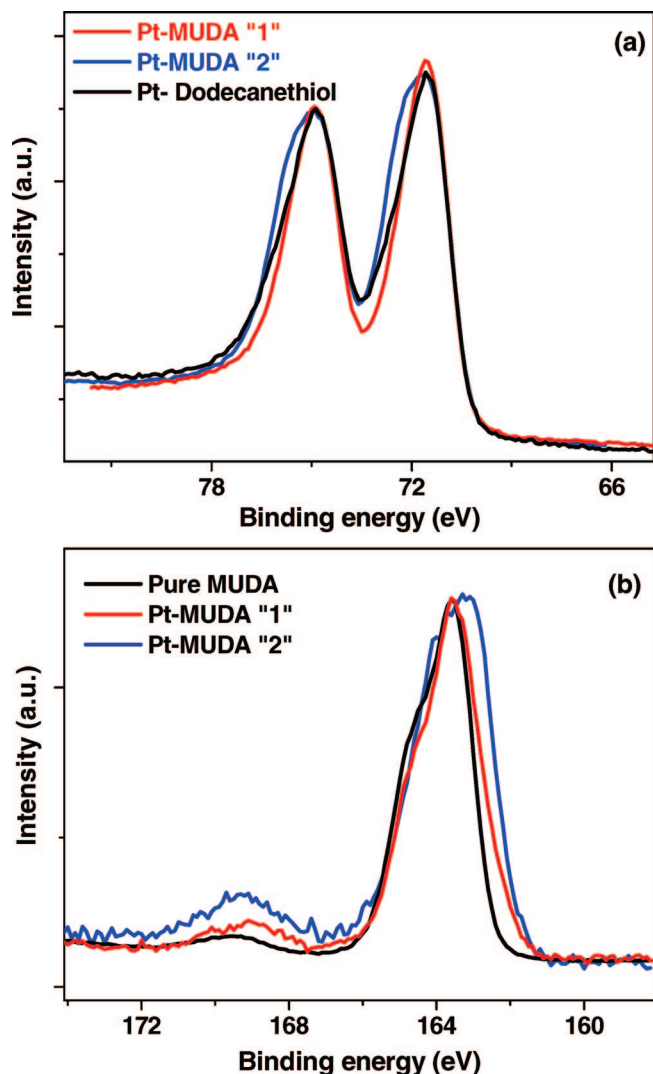


Figure 5. X-ray photoelectron spectra of MUDA-coated platinum particles showing the Pt 4f region (a) and the S 2p region (b). The two Pt-MUDA 1 and 2 samples differ in the contact between MUDA and the particles, 1 night and several days, respectively, before the XPS spectrum was recorded.

one (noted Pt-MUDA 2), these two steps have been extended to several days. The XP spectrum of pure MUDA was also recorded as a reference. For pure MUDA and for both samples, the C 1s peak contains three contributions at binding energies of 289.4, 287.0, and 285.0 eV with respective intensities of 1:1:9. These binding energies have been attributed, respectively, to the carbon of the acid carboxylic function, to the one in the α position with respect to sulfur, and to the nine carbon atoms of the alkyl chain as expected for MUDA. This result shows that the organic part of these samples is MUDA whatever the contact time. In both samples, MUDA and platinum particles coprecipitated.

Nevertheless, the Pt and S binding energies depend strongly on the contact time. For the freshly functionalized Pt-MUDA 1 powder, the Pt 4f_{7/2} peak presents only one contribution at a binding energy of 71.5 eV corresponding to platinum in the zero-valent state. For the Pt-MUDA 2 sample, an additional contribution at 72.5 eV could be detected (Figure 5a). This one is attributed to Pt^{δ+} species that can be platinum atoms bonded to sulfur as in the case of dodecanethiol-functionalized particles. The S 2p_{3/2} binding energy of the freshly functionalized Pt-MUDA 1 particles is very close to that of the free MUDA reference molecule (Figure 5b) with the main contribution at 163.5 eV.

This energy is generally attributed either to the thiol function or to disulfide species.³⁷ For the Pt-MUDA 2 sample, simultaneously with the blue shift of the Pt 4f_{7/2} peak described above, the main S 2p peak is enlarged and red-shifted (Figure 5b). This peak results from two contributions. The first one is characteristic of sulfur belonging to MUDA molecules in weak interactions with the nanoparticles. The binding energy of the second one is located at 163.0 eV and reveals charge transfer from platinum to sulfur, highlighting the Pt^{δ+}–S^{δ-} MUDA chemical bond. Several XPS studies on self-assembled monolayers of thiols on platinum film revealed the formation of Pt–thiolate bonding with an S 2p_{3/2} binding energy of 162.5 eV.^{38,39} This slight difference in BE can be due to the coordination mode of sulfur atoms that may be very different on a smooth Pt layer and on 2 nm Pt particles presenting a very high proportion of Pt atoms occupying kinks and edges. Table 1 reports the binding energies and the proportion of each component extracted from the fitting of the Pt 4f and S 2p signals. For the Pt-MUDA 2 sample, the proportion of platinum bound to a sulfur atom reaches a value that is very similar to that observed in dodecanethiol-coated particles, and the main part of the MUDA molecules are bound to the platinum particles. On the contrary, it is observed that despite the coprecipitation of MUDA molecules and platinum particles in the Pt-MUDA 1 sample, MUDA and particles interact very weakly. This study shows that the Pt–S bonding of the thiol groups in the mercaptoacid molecules occurs very slowly.

Finally, it must be noted that an additional contribution of weak intensity at 169.0 eV attributed to sulfonate impurities²⁶ is observed in the MUDA precursor as well as in the colloid powders (Figure 5b).

Infrared Spectroscopy. The ATR-FTIR spectrum of platinum particles deposited on a polyol solution on a silicon wafer is presented Figure 6a. It displays a very broad signal at 3280 cm⁻¹ due to the stretching vibration of the hydroxo groups and two bands at 2928 and 2882 cm⁻¹ corresponding to the ν (CH) vibrations of CH₂ groups of ethanediol. Intense signals are also observed corresponding to the antisymmetric ν (CO) stretching vibration of carboxylic acid groups and to carboxylate groups at 1741 and 1615 cm⁻¹, respectively. These latter correspond to the acetate ions added to the polyol for the reaction. The former can correspond to acetic acid resulting from proton exchange with the polyol and also to formic acid resulting from ethanediol oxidation.⁴⁰

Among all these groups corresponding to molecular species present in the polyol solution, a small peak is also evidenced at 2033 cm⁻¹ that is attributed to the vibrational frequency of on-top adsorbed CO molecules (Figure 6a). This is evidence that CO is produced during the reaction and is trapped on the platinum particle surface. The stretching vibration of CO molecules on Pt surfaces is generally found between 2060 and 2100 cm⁻¹, depending mainly on the surface coverage. Several studies reported on the blue shift of the CO stretching frequency with increasing surface coverage by varying the CO partial pressure.⁴¹ This phenomenon is attributed to a variation of dipole coupling with CO density.^{41,42} On corrugated (335) Pt surfaces, the band at 2059 cm⁻¹ was attributed to CO adsorbed on the terraces, and

(37) (a) Volmer, M.; Stratmann, M.; Viehhaus, H. *Surf. Interface Anal.* **1990**, *16*, 278. (b) Bain, C. D.; Biebuyck, H. A.; Whitesides, G. M. *Langmuir* **1989**, *5*, 723.

(38) Li, Z.; Chang, S.-C.; Williams, R. S. *Langmuir* **2003**, *19*, 6744.

(39) Laiho, T.; Leiro, J. A. *Appl. Surf. Sci.* **2006**, *252*, 6304.

(40) Blin, B.; Fiévet, F.; Beaupère, D.; Figlarz, M. *New J. Chem.* **1989**, *13*, 67.

(41) Crossley, A.; King, D. A. *Surf. Sci.* **1977**, *68*, 528.

(42) Urakawa, A.; Bürgi, T.; Schlöpfer, H.-P.; Baiker, A. *J. Chem. Phys.* **2006**, *124*, 054717.

Table 1. Pt 4f_{7/2} and S 2p_{3/2} Binding Energies and Relative Proportions of Each Component Measured by XPS^a for Two MUDA-coated Platinum Particles Depending on the Contact Time between MUDA and Particles

sample	Pt 4f _{7/2}			S 2p _{3/2}			
	Pt 4f _{7/2} (eV) 1	Pt 4f _{7/2} (eV) 2	Pt ₍₁₎ /Pt ₍₂₎ (%)	S 2p _{3/2} (eV) 1	S 2p _{3/2} (eV) 2	S 2p _{3/2} (eV) 3	S ₍₁₎ /S ₍₂₎ /S ₍₃₎ (%)
MUDA					163.6 (1.3)	169.3 (1.4)	0/96/4
Pt-MUDA 1	71.5 (1.5)		100/0		163.4 (1.6)	168.8 (1.5)	0/93/7
Pt-MUDA 2	71.4 (1.5)	72.5 (1.5)	70/30	163.0 (1.3)	163.8 (1.4)	168.8 (1.6)	64/26/10

^a fwhm values are given in parentheses.

the band at 2009 cm⁻¹ was attributed to CO adsorbed on the edges.⁴³ When it is adsorbed on Pt nanoparticles, the $\nu(\text{CO})$ energy of carbon monoxide varies with the particle size and surface state. On 7 nm cubic particles coated with PVP, this frequency was found to be between 2065 and 2085 cm⁻¹ depending on O₂ pretreatment.⁴⁴ This vibrational frequency has been observed at 2050 cm⁻¹ on ca. 1.5 nm Pt nanoparticles prepared by the reduction of Pt₂(dba)₃ under 1 bar of carbon monoxide.¹¹ The $\nu(\text{CO})$ energy measured on Pt particles prepared in polyol is out of the range usually observed (except for that in ref 43). This shift can be explained by very low CO surface coverage. Indeed, contrary to the experiments cited previously for which the IR spectra were recorded under CO partial pressure, in our case carbon monoxide is produced in situ by polyol oxidation and is certainly at a much lower concentration. As a matter of fact, this band is shifted to 2046 cm⁻¹ when the particles are exposed to a CO pressure of 1 bar.

The most striking feature of the ATR-FTIR spectra of particles coated with dodecylamine and dodecanethiol is the red shift of the on-top-adsorbed CO vibration, from 2033 to 2024 cm⁻¹ for the amine-coated particles and up to 1997 cm⁻¹ for the thiol-coated particles (Figure 6b). This shift can be attributed (i) to a decreasing CO covering rate by displacement with the coordination of dodecanethiol as was stated previously⁴¹ and (ii) to an electronic enrichment of the particle due to the ligands. This latter effect was considered to explain the shift of $\nu(\text{CO})$ to 2039 cm⁻¹ for platinum nanoparticles with thiol functionalization.¹¹ In both cases, this red shift is a good indicator of the coordination of the ligands at the surface of the particles. It is interesting that the red shift is much lower for the amine-coated particles, which shows that the electronic effect induced by the coordination of amine is very different from that induced by thiol and/or that the degree of functionalization is lower. This observation is in good agreement with the XPS results.

The other peaks in the FTIR spectrum of dodecanethiol-coated particles are attributed to the stretching vibration $\nu(\text{CH})$ of the CH₃ group of dodecanethiol at 2955 cm⁻¹, to the antisymmetric and symmetric $\nu_{\text{as}}(\text{CH})$ and $\nu_{\text{s}}(\text{CH})$ vibrations of the CH₂ groups at 2923 and 2853 cm⁻¹, respectively, and to bridging adsorbed CO at 1782 cm⁻¹ (Figure 6b). The position of the $\nu_{\text{as}}(\text{CH})$ signal of long-chain thiol assembled onto a surface is found to be in the range of 2925–2916 cm⁻¹ depending on the chain conformation. The higher value corresponds to molecules in the disordered liquid state, and the lower one corresponds to crystallized species presenting an all-trans configuration. In self-assembled monolayers, significant red shifts are observed with good organization. The position of the $\nu_{\text{as}}(\text{CH})$ signal at 2923 cm⁻¹ for the thiol-capped particles indicates a lower level of gauche defects with respect to liquid as a result of interactions between the alkyl chains and suggests a partial self-assembly process. However, the level of organization observed on planar Pt substrates is not attained. The peak corresponding to the carboxylate ions observed

in the raw particles has disappeared. Such an observation has already been made with ruthenium particles prepared in acetate solution in polyol and subsequently coated by thiols: the grafting of thiols and the extraction in a hydrophobic medium such as toluene remove the acetate ions from the particle surface.⁴⁵ Nevertheless, a small peak remains at 1731 cm⁻¹ indicating that some carboxylic acid molecules are strongly bound to platinum particles.

The functionalization of platinum particles by MUDA was also followed by FTIR spectroscopy. A typical spectrum of particles coated with MUDA and deposited on a silicon wafer is presented Figure 6c. As in the case of dodecylamine- and dodecanethiol-coated particles, carbon monoxide is still present at the surface of the particles. The on-top-adsorbed CO stretching vibration $\nu(\text{CO})$ appeared in the range of 2018–2002 cm⁻¹ and varied with the degree of functionalization. Indeed, the location of the CO band was found to depend on two parameters: the contact time of platinum particles with MUDA and the aging of the platinum particles in polyol before being functionalized with MUDA. For a given platinum colloidal solution, the on-top-adsorbed CO signal was red shifted to 2009, 2006, and 2003 cm⁻¹ by the respective contact of the silicon wafer with (i) 2 drops of a 10⁻⁴ M MUDA solution in ethanol, (ii) 4 more drops of 5 × 10⁻⁴ M MUDA solution in ethanol, and (iii) 2 more days of immersion in a 10⁻⁴ M MUDA solution in ethanol (Figure 7). Thus, a large excess of MUDA is necessary to reach an on-top $\nu(\text{CO})$ value similar to that measured on dodecanethiol-coated particles. This confirms the XPS study: the functionalization of platinum particles with MUDA is much slower than with dodecanethiol. Furthermore, when platinum particles have been stored in the polyol solution for about 2 weeks, the corresponding signal is located at 2010 cm⁻¹. When the delay between the synthesis and the functionalization was longer (about 2 months), then the $\nu(\text{CO})$ band was found to be at 2018 cm⁻¹. This dependence of $\nu(\text{CO})$ on the age of the platinum particles in polyol before functionalization is likely due to an enrichment of CO at the particle surface with time before functionalization. It certainly makes the subsequent grafting of MUDA more difficult because the thiol function must remove CO molecules that are strongly bounded to the surface of platinum particles.

The other peaks present on the IR spectrum of the MUDA-coated particles are the stretching vibrations $\nu_{\text{as}}(\text{CH})$ and $\nu_{\text{s}}(\text{CH})$ of the CH₂ groups at 2919 and 2851 cm⁻¹, respectively, the stretching vibration $\nu(\text{CO})$ of bridging CO at 1800 cm⁻¹, and the vibration of the carboxylic acid function of MUDA at 1736 and 1709 cm⁻¹ (Figure 6c). As in the case of particles coated with dodecanethiol, there is no remaining carboxylate peak in the IR spectrum. Acetate ions are removed by the coating and, in this case, by the washing with water, as well.

The 2919 cm⁻¹ energy value of $\nu_{\text{as}}(\text{CH})$ corresponds to MUDA molecules presenting a good organization with a nearly all-trans configuration of the alkyl chains, as in self-assembled monolayers.

(43) Shin, J.; Korzeniewski, C. *J. Phys. Chem.* **1995**, *99*, 3419.

(44) Kwestin, S. J.; Rioux, R. M.; Habas, S. E.; Komvopoulos, K.; Yang, P.; Somorjai, G. A. *J. Phys. Chem. B* **2006**, *110*, 15920.

(45) Chakroune, N.; Viau, G.; Ammar, S.; Veautier, D.; Poul, L.; Chehimi, M. M.; Mangeney, C.; Villain, F.; Fiévet, F. *Langmuir* **2005**, *21*, 6788.

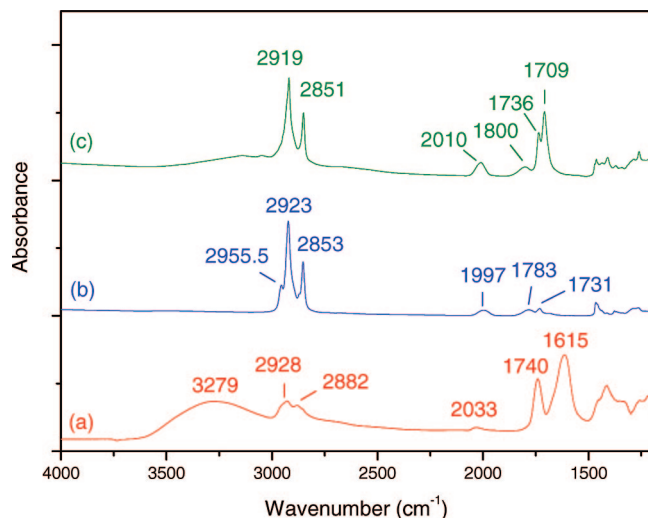


Figure 6. FTIR spectrum of 1.7 nm platinum (a) extracted from polyol, (b) coated with dodecanethiol, (c) and coated with MUDA. One drop of solution was deposited on a silicon wafer, and the spectra were recorded after the evaporation of the solvent.

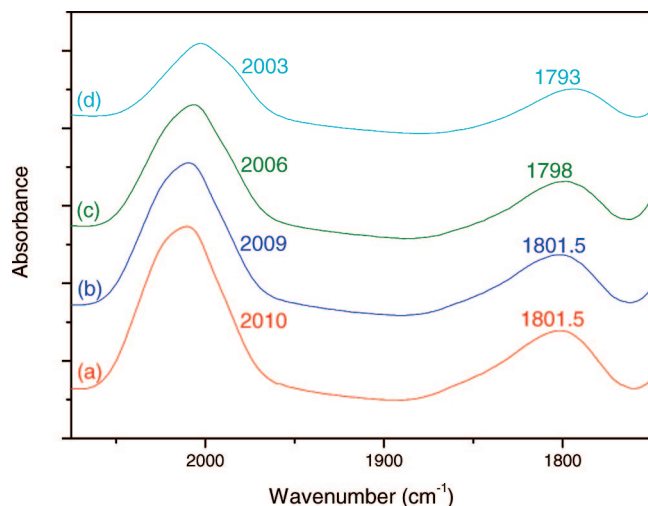


Figure 7. Influence of contact time of MUDA with Pt nanoparticles on CO stretching vibrational energy: (a) Pt nanoparticles washed three times for 5 min each in ethanol; (b) after the addition of 2 drops of a 10^{-4} M MUDA solution in ethanol; (c) after the addition of 4 more drops of a 5×10^{-4} M MUDA solution in ethanol; and (d) after 2 days in a 10^{-4} M MUDA solution in ethanol.

This organization is attributed to the excess free molecules crystallizing on the silicon wafer after the evaporation of ethanol. After the ethanol wash, the $\nu_{\text{as}}(\text{CH})$ peak is shifted to 2924 cm^{-1} , showing that when the free molecules are removed the MUDA remaining at the surface of the Pt particles does not present better organization than do dodecanethiol molecules. This observation confirmed that the amount of MUDA in strong interaction with the particles is much lower than the amount of dodecanethiol. Schmitt et al. observed a better organization of 8-mercapto-1-octanoic acid on 3.3 nm gold particles.⁴⁶ Two points can be put forward to explain this difference. First, on larger particles the faces are more developed, favoring interactions between alkyl chains. On the contrary, in the case of 1.7 nm particles the surface evidenced by PDF analysis precludes organization. Second, the density of mercaptoacid coating the particles was certainly higher in the case of gold particles than in this study because of the CO molecules that block some adsorption sites and hinder the functionalization.

The two peaks at 1736 and 1709 cm^{-1} are attributed to the carboxylic groups that are and are not involved in hydrogen bonding, respectively. The intensity of these peaks is much higher than that observed on the dodecanethiol-coated particles and belongs mainly to the MUDA molecules. The peak at 1709 cm^{-1} shows that an important part of the acid groups of MUDA are involved in hydrogen bonding. Two kinds of hydrogen bonds can be considered: lateral hydrogen bonds between acid functions of MUDA molecules linked to the same particle and axial hydrogen bonds between acid functions of MUDA molecules linked to two different particles.⁴⁶ The first ones are expected to present a stretching vibration at 1718 cm^{-1} , and the second ones, at 1708 cm^{-1} .⁴⁷ The intense peak located at 1709 cm^{-1} indicates that in our case the predominant hydrogen bonds are axial rather than lateral. This is in agreement with poorly organized molecules at the particle surface and with a low density of adsorbed MUDA. These hydrogen bonds well explain the formation of small aggregates of particles.

Interaction of Pt-MUDA Particles with Alumina Surfaces.

The alumina surfaces were immersed in a solution containing platinum nanoparticles coated with MUDA for 1 night and then washed abundantly with ethanol. To improve washings, alumina-covered silicon wafers have been sonicated in ethanol.

TEM. After the immersion of alumina membranes in colloidal solutions containing MUDA-coated particles, the particle density retained at the surface was found to increase significantly with the 98% H_2SO_4 pretreatment, the immersion time length, and the particle concentration. This is illustrated by the TEM images presented in Figure 8. For the same particle concentration (2.4×10^{-3} M in atomic platinum) and the same immersion time (16 h), without H_2SO_4 pretreatment only aggregates of particles are adsorbed on the alumina membrane (Figure 8a) whereas the 98% H_2SO_4 treatment favors the adsorption of isolated particles and increase the particle density (Figure 8b). As previously described,⁴⁸ the sulfuric acid plays the role of an alumina cleaner: by removing adsorbed contaminant species, it allows an increase in the immobilization yield of the particles. The immersion in a more concentrated solution (3.9×10^{-3} M) for the same time mainly favors the adsorption of aggregates of particles (Figure 8c). We think that increasing the particle concentration increases the number of these aggregates in solution. With a lower particle concentration, increasing the immersion time length to 48 h fully saturated the alumina membrane.

XPS. A silicon wafer covered with a 6-nm-thick alumina layer and treated with 98% sulfuric acid was immersed for 1 night in a 2.4×10^{-3} M (in atomic platinum) ethanol solution of MUDA-coated platinum particles and then washed three times in ethanol. The XPS survey spectrum displayed in Figure 9 shows the presence of Pt, C, and S signals due to the nanoparticles, together with that of Al and O due to the substrate. Additional signals attributed to chlorine and nitrogen are observed. Whereas chlorine may come from HCl solution, the origin of nitrogen that is also found in the survey of pure MUDA (not shown) is unknown. The high-resolution Pt 4f, C 1s, and S 2p spectra appear to be very similar to that of MUDA-coated Pt particles, thus evidencing the effective immobilization of the particles at the alumina surface. Particularly considering the S 2p signal, it was compared in the inset of Figure 9 with that for Pt-MUDA 1 and 2 samples presented in the previous section. One observes clearly a high similarity

(46) Schmitt, H.; Badia, A.; Dickinson, L.; Reven, L.; Lennox, R. B. *Adv. Mater.* **1998**, *10*, 475.

(47) Smith, E. L.; Alves, C. A.; Andereg, J. W.; Porter, M. D.; Siperko, L. M. *Langmuir* **1992**, *8*, 2707.

(48) Kalb, W.; Lang, P.; Mottaghi, M.; Aubin, H.; Horowitz, G.; Wuttig, M. *Synth. Met.* **2004**, *146*, 279.

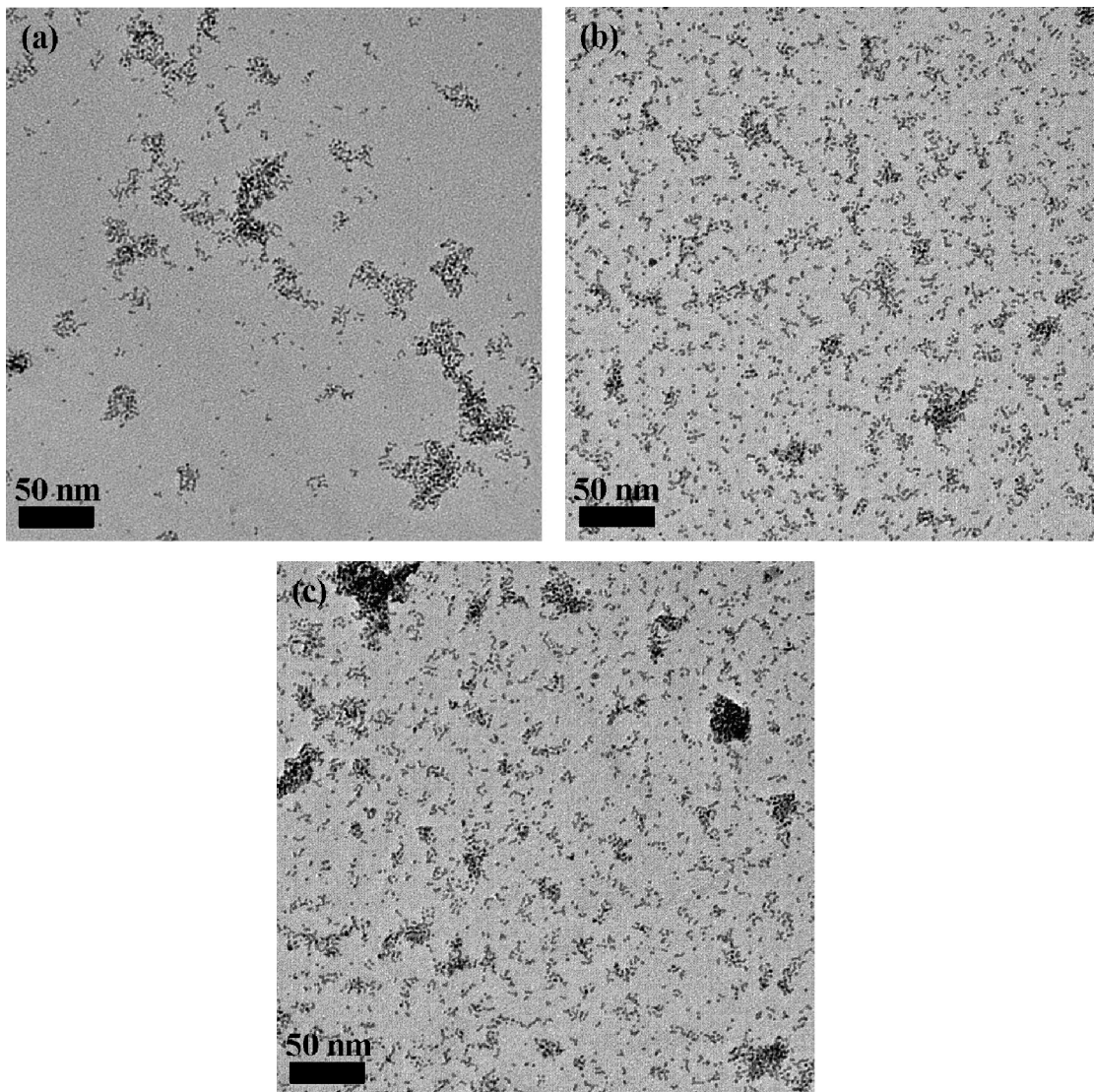


Figure 8. TEM images of 3-nm-thick alumina membranes deposited on a copper grid and immersed in a colloidal solution containing MUDA-coated platinum nanoparticles showing the influence of the Al_2O_3 surface state and the solution concentration on the density of immobilized particles at the surface after 16 h of immersion: (a) no H_2SO_4 pretreatment, (b, c) 98% H_2SO_4 pretreatment; (a, b) 2.4×10^{-3} M and (c) 3.9×10^{-3} M in atomic platinum.

between the S 2p signal obtained on modified-alumina surfaces and that of particles that have been in contact with MUDA for a long time, in the presence of a component at ca. 163 eV corresponding to thiolate–Pt species. It shows that the main part of the particles retained at the surface after washing with ethanol are linked to the sulfur atom of the MUDA and present dangling carboxylic acids.

FTIR. An ATR-FTIR silicon wafer covered with a 6-nm-thick alumina layer and treated with 98% sulfuric acid has been immersed for 1 night in a 2.4×10^{-3} M (in atomic platinum) ethanol solution of MUDA-covered platinum particles and then washed twice with 2 mL of ethanol. On the resulting spectrum, the $\nu_{\text{as}}(\text{CH})$ and $\nu_{\text{s}}(\text{CH})$ signals are observed at 2924 and 2852 cm^{-1} , and the on-top and bridging adsorbed CO signals are observed at 2016 and 1801 cm^{-1} (Figure 10a). The bands at 1733 and 1708 cm^{-1} correspond to the MUDA carboxylic group that are not involved and involved in axial hydrogen bonding, respectively.

The alkyl chains of the MUDA molecules are poorly organized on alumina as inferred from the energy of the $\nu_{\text{as}}(\text{CH})$; consequently, the free molecules were easily removed from the

substrate by washing with ethanol. The comparison with the spectrum of particles deposited on a silicon wafer that have not been washed (Figure 6c) also shows that the $\nu(\text{CO})/\nu(\text{CH}_2)$ intensity ratio is much higher in spectrum 10a. If we consider that the $\nu(\text{CO})$ intensity is characteristic of the platinum particles and that the $\nu(\text{CH})$ intensity characterizes whole MUDA molecules (free molecules and those grafted to the particles), then a higher $\nu(\text{CO})/\nu(\text{CH}_2)$ ratio favors a higher proportion of coated particles with respect to free molecules.

Immobilization on alumina and silica surfaces has been compared. For that, a silicon wafer has been immersed in an MUDA-coated particle colloidal solution under the same conditions. We have estimated the number of platinum particles immobilized on both surfaces by integrating their $\nu(\text{CO})$ signal on the two spectra recorded after brief washing with ethanol, considering that the intensity of this signal accounts for the particle density at the surface. The $\nu(\text{CO})$ signal on alumina was found to be about 6 times more intense than the corresponding peak on silica. Thus, a stronger interaction of MUDA-coated particles with alumina than with silica is inferred. This result can be explained by ionic carboxylate bonds between MUDA and the

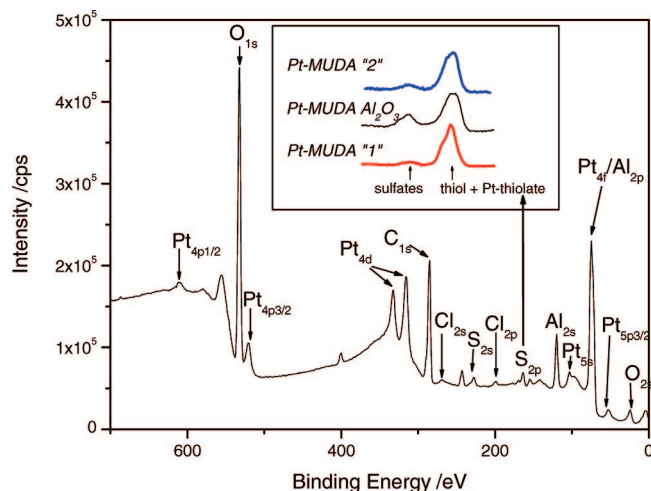


Figure 9. XPS survey spectrum of PtMUDA nanoparticles immobilized on Al_2O_3 by the immersion of an alumina substrate in a HCl/ethanol colloidal solution and then washing abundantly with ethanol. The inset shows the S 2p high-resolution spectrum (black) in comparison with the spectra of samples Pt-MUDA 1 and 2 (red and blue lines, respectively).

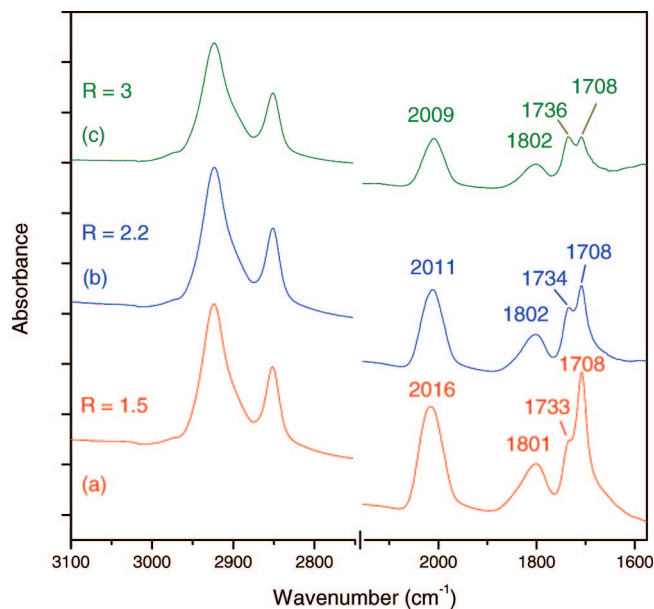


Figure 10. Influence of washing on IR spectra of PtMUDA nanoparticles immobilized on Al_2O_3 : (a) twice with 2 mL of ethanol, (b) three times for 5 min and twice for 5 min of sonication in ethanol, and (c) for an additional 15 min of sonication in ethanol. The intensity ratio $R = I(\nu_{\text{as}}(\text{CH}))/I(\nu(\text{CO}))$ was found to increase steadily with washing.

protonated alumina surface⁴⁹ whereas only Hamaker interactions take place with silica. In the case of ionic interaction between carboxylate functions and the protonated alumina surface, one would expect the evidence of carboxylate groups in the IR spectrum. Actually, a broad band is observed in the region around 1460 cm^{-1} in which the $\nu_{\text{s}}(\text{CO})$ of carboxylate groups is expected. Unfortunately, this band can be due to other contributions such as $\delta(\text{CH}_2)$ or $\nu_{\text{s}}(\text{CO})$ of carbonate groups of a surface contaminant. As a consequence, the detection of the carboxylate groups was very difficult; therefore, the expected intensity of this band should be quite low relatively to the $\delta(\text{CH}_2)$ of all of the alkyl chains.

Extensive washings (i) three times for 5 min and twice for 5 min of sonication and (ii) for an additional 15 min of sonication

in ethanol indicate that the interaction between the particles and the support is strong. Actually, the additional 15 min of sonication is necessary to observe significant decreases in the $\nu(\text{CH})$ and $\nu(\text{CO})$ peak intensities (Figure 10c).

Another fact that appears during washing is the relative increase in the peak located at 1733 cm^{-1} (free COOH) with respect to the one at 1708 cm^{-1} (COOH in dimer) (Figure 10). This shows that the carboxylic groups involved in hydrogen bonding are preferentially eliminated and suggests that the aggregates that were observed in TEM images are made up of particles linked with each other by hydrogen bonding and are eliminated first with sonication. We conclude that the less interconnected NPs interact strongly with the Al_2O_3 surface.

The last process observed with extensive washings is the shift of the on-top-adsorbed CO band from 2016 to 2009 cm^{-1} (Figure 10). We have concluded in the previous section that the energy of the on-top CO vibration was dependent on the degree of functionalization. Consequently, everything seems to happen as if the less-MUDA-functionalized particles are eliminated before the others. This observation is confirmed by the variation of the intensity ratio $\nu_{\text{as}}(\text{CH})/\nu(\text{CO})$. It increases steadily with washing from 1.5 to 3 (Figure 10) and shows that the particles that remain on the alumina surface after extensive washing contain more MUDA molecules. In conclusion, IR spectroscopy allows us to conclude that the particles that are eliminated first with ethanol washing are (i) the less-functionalized particles and (ii) the particles forming aggregates by hydrogen bonds, which are not bonded or are weakly bonded to the Al_2O_3 substrate. These conclusions are illustrated in Figure 11.

Summary

Platinum particles (1.7 nm in size) were synthesized by the reduction of platinum salts in 1,2-ethanediol and subsequently coated with dodecylamine, dodecanethiol, or ω -mercaptoundecanoic acid (MUDA). These particles are crystalline with an fcc-type structure with structural disorder inherent for such particles presenting a very high surface/volume ratio. XPS and FTIR were also very efficient techniques to give a clear description of both the particle functionalization and immobilization on an alumina surface.

XPS spectra showed that the platinum particles contain mainly Pt atoms in the zero-valent state. The structure of the particles was only slightly changed by functionalization by amine or thiol, but strong differences were inferred from the XPS spectra. Indeed, although no electronic effect was observed on dodecylamine-coated particle spectra, on thiol-coated particle spectra, platinum-to-sulfur charge transfer provokes a concomitant shift of the Pt 4f and S 2p binding energy toward high and low energy, respectively. The formation of a $\text{Pt}^{\delta+}-\text{S}^{\delta-}$ bond is thus evidenced. XPS also showed that functionalization with MUDA is slower than with dodecanethiol because the largest contact time between MUDA and the particles is necessary to record a significant energy shift in the XPS spectra.

FTIR spectra of raw platinum particles showed carbon monoxide and carboxylate ions at their surfaces. The carboxylate ions are the acetate added to polyol to favor particle stabilization. The CO molecules result from the polyol oxidation. After functionalization either by dodecanethiol or by MUDA, the carboxylate ions are totally removed from the particle surface whereas the band of CO remains in the IR spectra. A shift of the stretching vibration $\nu(\text{CO})$ toward low energy is observed with functionalization. The importance of the red shift depends on the molecule grafted at the particle surface in the following order: dodecanethiol > MUDA > dodecylamine. This red shift is assigned to the decreasing CO density at the surface and to

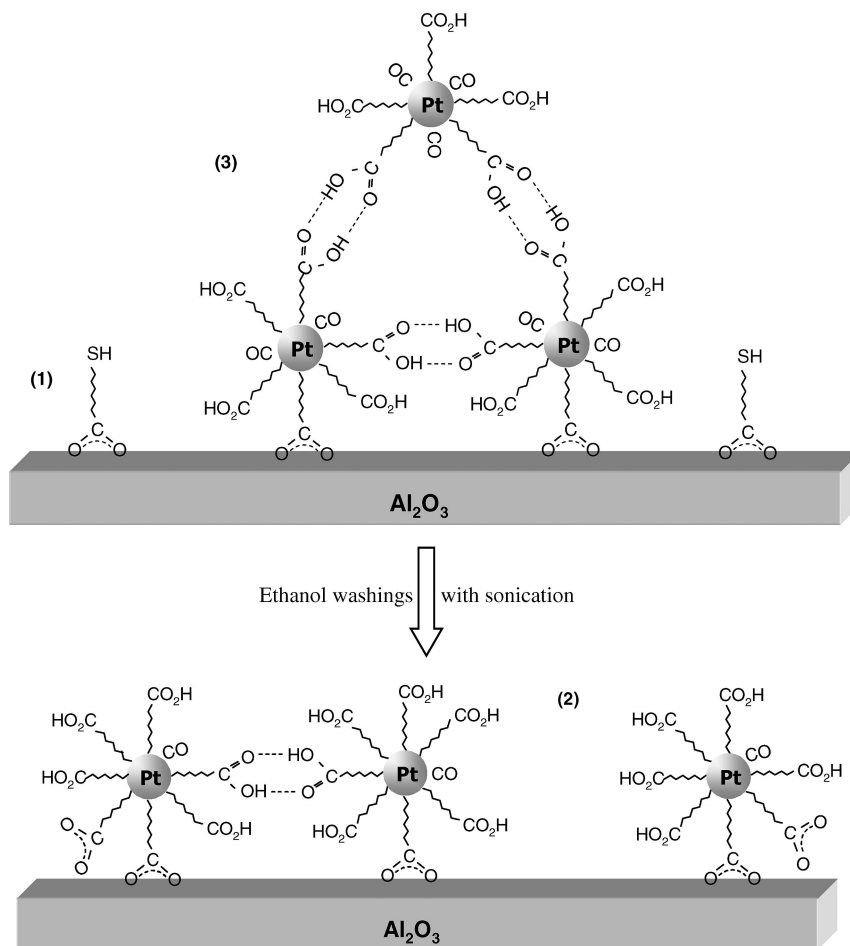


Figure 11. Ideal representation of the different species immobilized on the alumina surface after immersion in a colloidal solution containing Pt-MUDA particles: (1) free MUDA molecules, (2) isolated or quasi-isolated particles, and (3) aggregates of particles interconnected by hydrogen bonds. The free molecules (1) are very easily removed from the surface by washing, and the aggregates (3) are removed by sonication. The particles undergoing strong interaction with the surface are those that present the highest degree of functionalization by MUDA molecules (2).

electronic effects resulting from the Pt–ligand chemical bond. Different electronic effects are expected for thiol and amine, explaining the different shifts. The $\nu(\text{CO})$ band was always found to be more red-shifted for dodecanethiol-coated particles than for MUDA-coated particles, showing that the functionalization with MUDA was less effective, in agreement with XPS. A large excess of MUDA is necessary to attain the degree of functionalization observed with dodecanethiol. The analysis of the location of the $\nu(\text{CO})$ band also revealed that the aging of platinum particles in polyol makes further functionalization with MUDA more difficult because of the surface enrichment in CO. In conclusion, the CO red shift appears to be an efficient probe of the density of adsorbed thiols on nanoparticles.

On dodecanethiol-coated particles, the stretching vibration $\nu_{\text{as}}(\text{CH})$ energy shows the partial self-assembly of the alkyl chains. Nevertheless, this organization is quite weak because of the very small size of the particles and also because of the presence of CO at the particle surface hindering the functionalization by the thiol groups. The poorest organization of the MUDA alkyl chains is even observed on MUDA-coated particles, which is likely due to the lower density of alkyl chains at the particle surface and also the terminal carboxylic acid groups that are involved in axial hydrogen bonds. These bonds are responsible for the interparticle interactions that originate in 3D aggregates.

Alumina substrates (membranes and thin layers) were immersed in colloidal solutions of MUDA-coated Pt particles. The particle density at the surface increases with sulfuric acid

pretreatment, immersion time, and particle concentration. Furthermore, the particle density on the surface of alumina thin layers was found to be higher than on the native silica layer on silicon, showing the specific interaction of MUDA-coated particles with alumina. XPS of the particles immobilized on the alumina surface showed a $\text{Pt}^{\delta+}-\text{S}^{\delta-}$ bond indicating that the interaction with alumina involves the dangling carboxylic groups. Isolated particles and 3D aggregates are observed on alumina membranes by TEM. On the thicker alumina layers, for which TEM is not efficient, IR spectroscopy revealed that washing by sonication performs an efficient sorting by first removing the free MUDA molecules and then preferentially the hydrogen-bonded particles in 3D aggregates rather than the quasi-isolated particles that undergo stronger interaction with the surface.

Acknowledgment. We thank N. Lidgi-Guigui and P. Seneor (UMP Thales-CNRS-Université Paris 11) for their help with the preparation of alumina thin layers by sputtering and Yang Ren, Argonne National Laboratory, for help with the high-energy XRD experiments. We acknowledge the French Ministry for Education and Research for financial support (ACI Nanoscience). The work was also supported in part by CMU through grant REF C602281. Use of the Advanced Photon Source was supported by the U.S. Department of Energy, Office of Science, Office of Basic Energy Sciences, under Contract No. DE-AC02-06CH11357.